

Cite this article as: Zhang Yuan, Yang Yuzhuo, Liu Yun, et al. Research Progress of Microstructure Characteristics and Mechanical Properties of Hot-Deformed Biodegradable Mg-based Alloys[J]. Rare Metal Materials and Engineering, 2024, 53(05): 1310-1320. DOI: 10.12442/j.issn.1002-185X.E20230027.

REVIEW

Research Progress of Microstructure Characteristics and Mechanical Properties of Hot-Deformed Biodegradable Mg-based Alloys

Zhang Yuan^{1,2}, Yang Yuzhuo¹, Liu Yun^{1,2}, Liu Wei¹, Tian Yaqiang^{1,2}, Chen Liansheng^{1,2}

¹School of Metallurgy and Energy, North China University of Science and Technology, Tangshan 063210, China; ²Key Laboratory of the Ministry of Education for Modern Metallurgy Technology, North China University of Science and Technology, Tangshan 063210, China

Abstract: Magnesium alloys offer a lot of potential in the biomedical fields, due to their suitable elastic modulus for human bone, spontaneous degradability, and excellent biocompatibility, while low absolute tensile or yield strength and barren plastic abilities at room temperature significantly restrict their applications. As a successful method of enhancing mechanical properties, the hot deformation process can not only refine the grain sizes and broken sediments, but also introduce the high-density dislocations and change the texture orientation to improve the strength and plasticity. Based on the microstructure evolution laws, the latest research progress of Mg-based alloys under various hot deformation processes was reviewed. The differences in the deformation methods of rolling, forging, extrusion, and high-pressure torsion were compared. Under various hot deformation methods, the mechanism of grain refinement and the impact of dynamic recrystallization and dislocation propagation on the mechanical properties of Mg alloys were discussed. In addition, the relationships between microstructure and mechanical properties of hot-deformed Mg alloys were summarized.

Key words: degradable Mg alloys; hot deformation; second precipitations; grain refinement; mechanical properties

Till now, the vascular stents and bone repair materials are commonly composed of inert titanium metal, stainless steel, Co-based, etc^[1-14]. However, these materials have potential safety risks such as stress-shielding effect, secondary operation, and toxic ions release^[15-21]. Fortunately, Mg-based alloys have received extensive attention in recent years, due to their excellent biocompatibility and spontaneous degradability^[22-31]. The specific application and evaluation methods of medical Mg in vivo/vitro are shown in Fig. 1^[32-36]. Regrettably, the weak mechanical strength and poor forming ability of Mg alloys easily result in automatic attenuation, ectopic torsional collapse, and even no-remonitory fracture^[37-39]. As a result, how to improve and match the mechanical properties of medical Mg alloys has become a key problem to be solved urgently.

More critically, the mechanical strength meeting the standards is the essential prerequisite and fundamental

guarantee for safe implantation and precision processing. Until now, the principal techniques for enhancing the mechanical properties of medical magnesium alloys are element micro-composite, heat treatment, hot deformation, etc^[40-42]. The element micro-composite can refine grain sizes and reduce the degree of segregation in unit volume. However, it induces large-scale low-temperature eutectic compounds at the triangular grain boundary, reducing the mechanical toughness and fatigue endurance of materials^[43-44]. The heat treatment can eliminate the solute segregations and improve strength through partial supersaturated solid solution precipitation. While, due to a long processing time, grain growth leads to the deterioration of material mechanical properties^[45-46]. Meanwhile, it is not easy to precisely control the grain sizes, morphology, and distribution of the second phases. The hot deformation can smash the continuous second phases and introduce high-density dislocations, which

Received date: August 31, 2023

Foundation item: Central Government Guided Local Science and Technology Development Fund Project (226Z1004G); Natural Science Foundation of Hebei Province (E2020209153); Open Fund of State Key Lab of New Metal Materials (2020-Z12); Science and Technology Project of Tangshan (20130205b)

Corresponding author: Liu Yun, Ph. D., Lecturer, Key Laboratory of the Ministry of Education for Modern Metallurgy Technology, North China University of Science and Technology, Tangshan 063210, P. R. China, Tel: 0086-315-8805420, E-mail: liuyun@ncst.edu.cn

Copyright © 2024, Northwest Institute for Nonferrous Metal Research. Published by Science Press. All rights reserved.

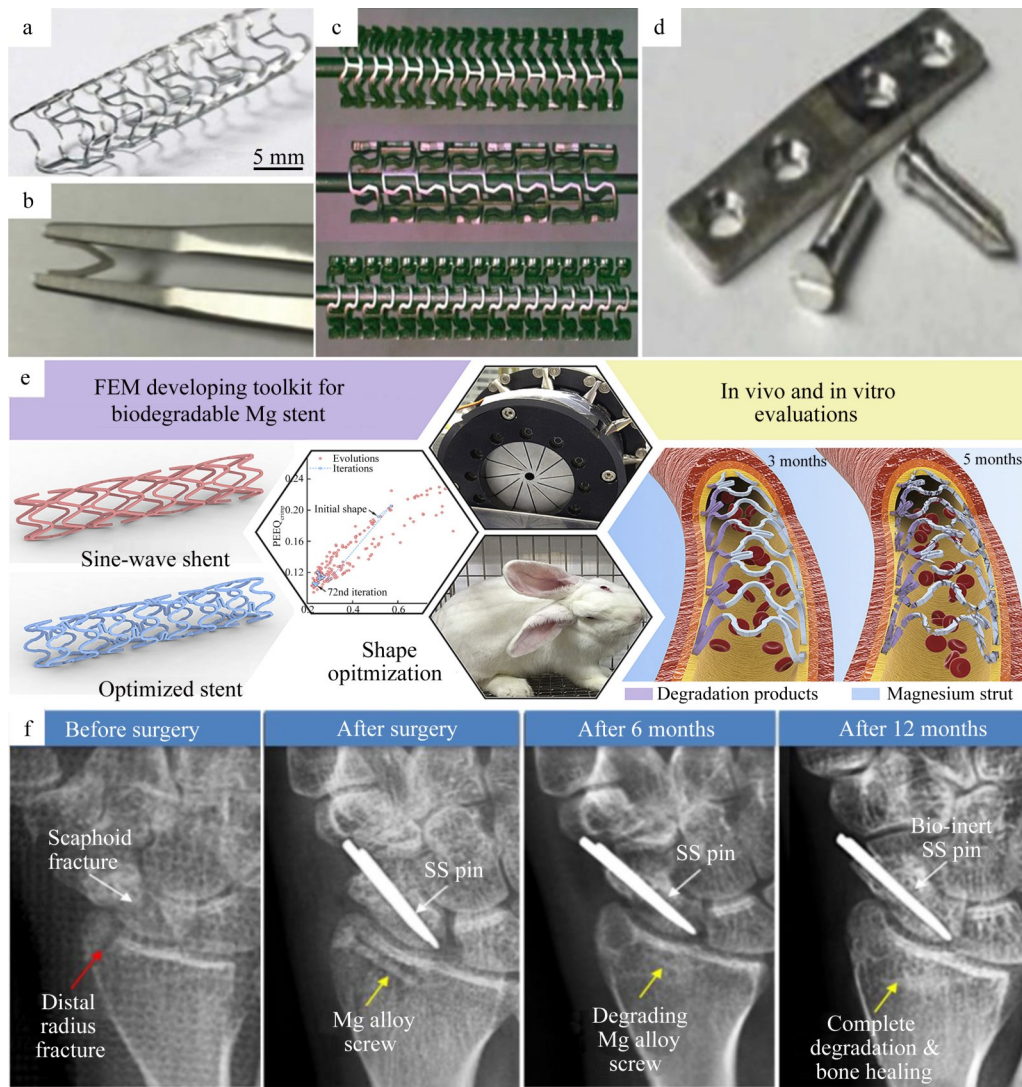


Fig.1 Application of medical Mg alloys in orthopedic devices (a)^[32], bone implant (b, d)^[33, 35], and vascular field (c)^[34]; biodegradable magnesium alloy in vitro and in vivo evaluation (e)^[36]; complete screw degradation and bone healing process (f)^[33]

improves the overall mechanical properties of the materials^[47-48]. In particular, the precipitation of ultra-fine nanocrystals and semi-coherent interfaces under large plastic deformation significantly enhance the strength and plasticity. It is also found that the multi-pass small deformation hot-rolling can significantly improve the mechanical characteristics of medical Mg/Zn-based alloys^[49-51]. In addition to ensuring the mechanical properties, its corrosion resistance is improved considerably.

Therefore, based on the microstructure evolution characteristics, the latest progress of medical Mg alloys is reviewed. Moreover, the grain refinement mechanism, dynamic recrystallization, and the impact of dislocation growth on the mechanical properties of medical Mg alloys under rolling, forging, extrusion, and high-pressure torsion processes are summarized and compared. The essential relationship between microstructure and mechanical properties of hot-deformed medical Mg alloys is further summarized. Finally, future development of medical magnesium alloys is reviewed.

1 Hot Deformation Classification

1.1 Rolling deformation

At present, rolling deformation is a widely used process in the precision forming of medical magnesium alloys, which can significantly improve the mechanical characteristics by eliminating the internal defects, pressing the internal structure, and refining the grains. In particular, high reductions and multi-pass rolling can further enhance the mechanical support of the implanted metal in the body. For example, Wang et al^[52] revealed the microstructural features and mechanical characteristics of biodegradable Mg-2Zn alloy. The results show that after different single-pass rolling treatments, the yield strength (YS) and ultimate tensile strength (UTS) increase from 78 and 126 MPa to 180 and 245 MPa, respectively, which is caused mainly by twin and dynamic recrystallization, leading to a considerable drop in grain size as rolling reduction increases. Thus, it can improve the strength of Mg-2Zn alloy. Meanwhile, Wang et al^[53]

investigated the microstructures and mechanical characteristics of the multi-pass rolled Mg-2.5Nd-0.5Zn-0.5Zr alloy. Research results reveal that after 3rd-pass, 311.9 MPa in UTS and 272.4 MPa in YS can be obtained, because the grain is refined throughout the multi-pass hot rolling, resulting in a small average grain size of 4.25 μm .

On this basis, Wang et al^[54] discussed the mechanical characteristic of medical Mg-2Zn alloy after multi-pass rolling with different degrees of deformation. Fig. 2 illustrates the grain refinement mechanism during rolling processes. It can be observed that when the rolling reduction increases from 50% to 91%, the third pass produces the nanocrystalline microstructure. The reason is that the twin-induced dynamic recrystallization is continuously improved. Meanwhile, results point out that with increasing the rolling reduction and rolling passes, the YS and UTS reach up to 223 and 260 MPa from 80 and 135 MPa, respectively. This is caused mainly by the continual grain refinement, which increases the alloy's strength. Meanwhile, the Zn segregation dramatically enhances the nanocrystal stability.

In addition to the effects of rolling pass and reductions on the mechanical characteristics of medical Mg alloy, the rolling temperature can also change its strength. For example, Liu et al^[55] investigated the mechanical attributes of sheets made of Mg-6Gd-1Er-0.5Zr at various rolling temperatures. The results point out that 367 MPa in UTS, 349 MPa in YS, and 9.1% in elongation can be achieved at 300 °C, showing the best mechanical properties. This is due to the production of the bimodal microstructure at 300 °C, which contains a lot of dislocations and equilibrium $\text{Mg}_5(\text{Gd}, \text{Er})$ precipitates. Thus, the alloy keeps a good strength-ductility balance. Deng et al^[56] investigated the impact of rolling treatment on the microstructural characteristics of WE43 alloy. The results show that in as-cast, cold-rolled, warm-rolled, and hot-rolled WE43 alloy, the YS is 99.8, 27.8, 327.5, and 178.4 MPa, and

UTS is 130.7, 284.1, 346.7, and 251.2 MPa, respectively, which is primarily due to the significantly refined alloy grains caused by increased rolling temperature. The as-cast alloy is composed of Mg_{24}Y_5 and a small amount of $\text{Mg}_{41}\text{Nd}_5$ phase. The $\text{Mg}_{41}\text{Nd}_5$ second phase precipitation and dispersion in the grain boundaries increase by dynamic recovery during hot rolling, which contributes to the strengthening effect of alloys.

Additionally, Mao et al^[57] studied the change of strength for the as-rolled biodegradable Mg-2Zn-0.05Ca. The findings demonstrate that the UTS and YS of rolled alloys dramatically reach 257 and 237.6 MPa, respectively. This is due to the fine single-phase grains formed after rolling. The solid-solution strengthening is another significant contributing factor to the increased strength. Furthermore, the rolled Mg-2Zn-0.05Ca demonstrates potential as medical implants by successfully balancing mechanical strength and corrosion resistance. Meanwhile, Gungor et al^[58] investigated the change of strength of the homogenized and hot-rolled Mg-3Zn-0.2Ca-0.3Mn alloy. Research results point out that after rolling, the YS changes from 57 MPa to 146 MPa, and UTS changes from 145 MPa to 229 MPa. However, the elongation is reduced from 7.0% to 1.6%. This is mainly because grain size decreases significantly, which promotes $\text{Ca}_2\text{Mg}_6\text{Zn}_3$ precipitation formation after rolling. Thus, the YS and UTS increase considerably. However, the increased densities of micro-cracks caused by more significant volume fraction of the $\text{Ca}_2\text{Mg}_6\text{Zn}_3$ phase harm or damage the elongation.

Compared with the standard rolling process, twin roll casting, as a cutting-edge international technology, can achieve better plate strength and elongation through a short process to avoid premature failure of implanted metal. For example, Hou et al^[59] discussed the in vitro evaluation on mechanical integrity of the twin roll casted (TRCed) ZX11 magnesium alloy. The findings demonstrate that the alloy after TRC has adequate mechanical strength with an increase in YS

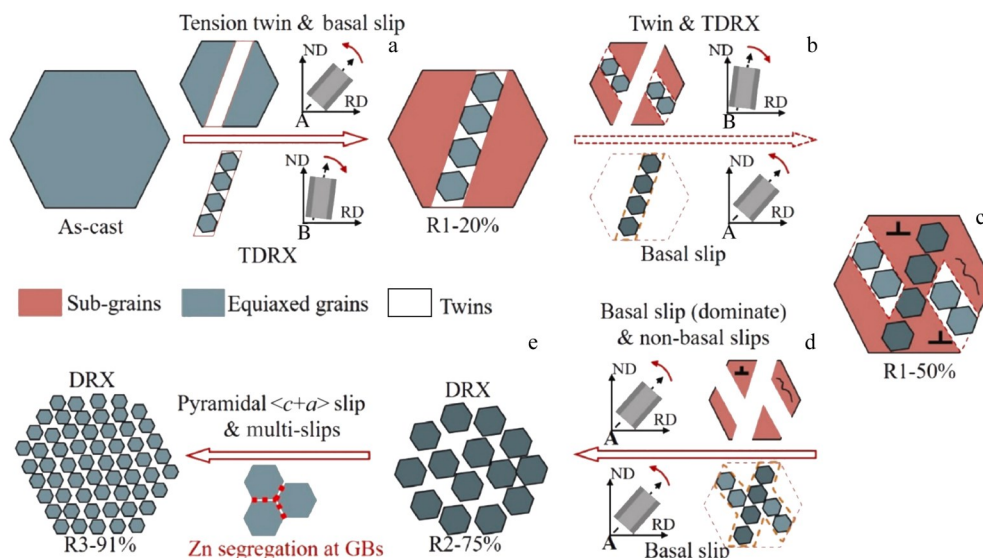


Fig.2 Schematic diagram for grains refinement of Z2 alloy during hot rolling^[54]

to 213 MPa and UTS to 256.2 MPa. This is because grain size decreases with TRC, and the strength of the alloy is enhanced by the interaction of dislocations with newly generated twin boundaries. Subsequently, Dargusch et al.^[60] assessed the mechanical characteristic of a TRCed rare earth-free Mg-Zn-Ca alloy. The results indicate that with good refinement (grain sizes below 150 μm), the TRCed Mg-0.5Zn-0.5Ca sheet displays UTS and elongation of 221.9 MPa and 9.3%, respectively. This is because the TRC process results in dynamic recrystallization. Thus, better grain refinement can be obtained, and the $\text{Ca}_2\text{Mg}_6\text{Zn}_3$ phase is concentrated along the grain boundaries. Thus, the mechanical properties are continuously improved. Moreover, the alloy with TRC may be used in cranial and maxillofacial fixation devices. The rolling process has the characteristics of mass production and high-performance production. Medical magnesium alloy implantation mainly aims at the profiles and plates required by specific position. However, it is rarely involved in some small complex components or special-shaped asymmetric structural parts.

1.2 Forging deformation

Compared with rolling, forging makes the internal structure of biomedical metals change significantly. After forging, the interior of the alloy becomes more compact, and the defects such as pore and shrinkage cavity are eliminated, which greatly improves the mechanical properties. In particular, the implanted metal after multi-pass and multi-direction forging has excellent development prospects in the biomedical field. For example, Duley et al.^[61] discussed the microstructural change of Mg-4Zn-0.5Ca-0.16Mn alloy with single-pass forging at different temperatures. The findings demonstrate that the alloy forged at 573 K has smaller deformed grains than at 523 or 623 K, and that the distribution of second phase

particle in the 573 K-forged alloy is evenner, because the forged alloy has a higher area proportion of dynamic recrystallization grains beyond expectation. On this basis, Duley et al.^[62] further verified the effect of annealing treatments on strength of forged Mg-4Zn-0.5Ca-0.16Mn alloy, as shown in Fig. 3; it shows that after forging followed by annealing for 5 min, the highest YS and UTS of 142 and 241 MPa can be obtained at 573 K, and the elongation is 20%, 15%, and 14% at three temperatures. According to Eq.(1–4), the total theoretically YS (σ_{theo}) can be calculated by the contributions of grain size (σ_{gs}), precipitates (σ_{ppt}), and dislocations (σ_{dis}). The highest YS and UTS are obtained at 573 K with annealing for 5 min, which is because of the high dislocation density, and the aggregation of precipitates. However, the oriented grains grow selectively at 573 K, which makes the grain size gradually uneven, so the elongation of the alloy decreases.

$$\sigma_{\text{gs}} = \sigma_0 + \frac{k}{\sqrt{d}} \quad (1)$$

$$\sigma_{\text{ppt}} = M \cdot \tau_{\text{CRSS}} = M \cdot \frac{G_b}{2\pi\sqrt{1-\nu}} \cdot \left(\frac{1}{\lambda^*}\right) \cdot \ln\left(\frac{d_{\text{p}^*}}{r_0}\right) \quad (2)$$

$$\sigma_{\text{dis}} = MaGb\sqrt{\rho} \quad (3)$$

$$\sigma_{\text{theo}} = \frac{k}{\sqrt{d}} + \sigma_{\text{ppt}} + \sigma_{\text{dis}} \quad (4)$$

Additionally, Merson et al.^[63] discussed the influence of multi-axial isothermal forging (MIF) on the mechanical properties of Mg-1Zn-0.2Ca alloy. It is indicated that after 5-passes forging at 300–400 °C, the YS reaches 100 MPa, the UTS reaches 200 MPa, and the elongation at break is improved by 14% up to 25%. This is due to the fact that after MIF processing, the alloy has a completely recrystallized

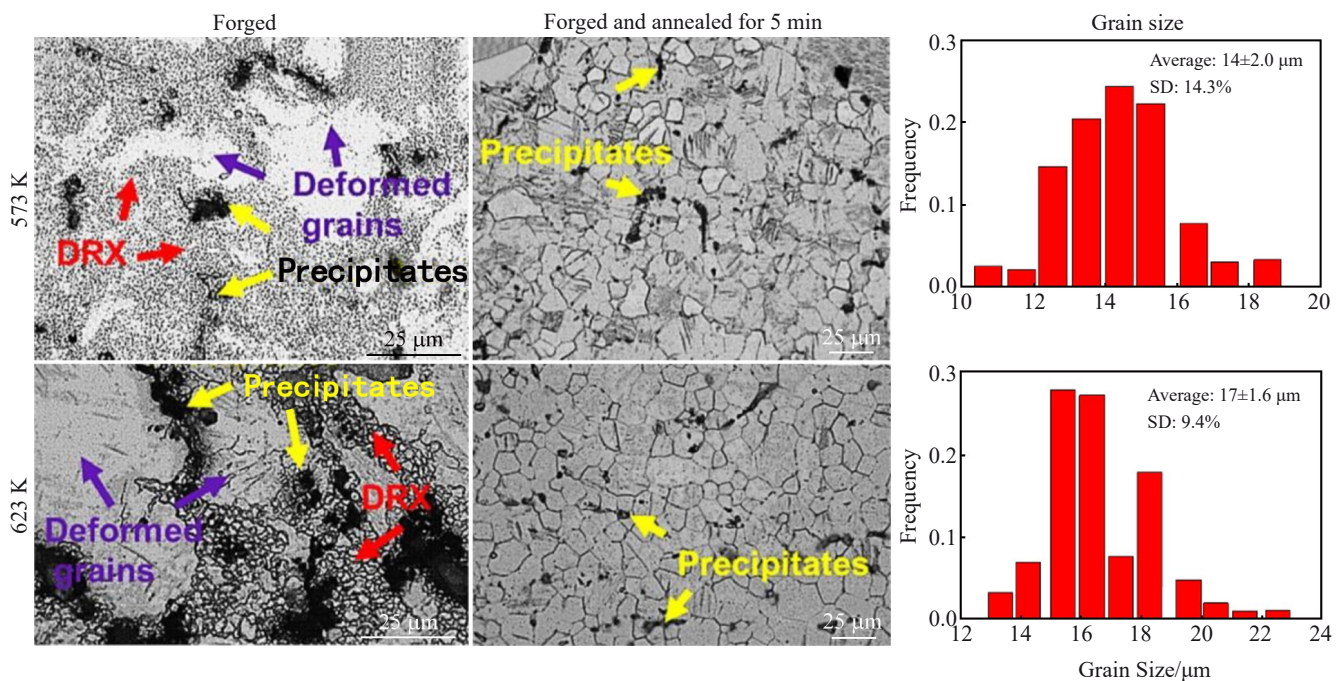


Fig.3 Optical microstructures and grain size distributions of the forged and annealed specimens^[62]

structure with the average grain size of 2.9 μm , so the strength and plasticity are significantly improved. Moreover, the MIF, followed by warm-rolling, can obtain an excellent balance between strength and flexibility.

Compared with the above methods, multi-directional forging (MDF) can not only save materials, but also make the structure more compact. For example, Ramesh et al^[64] discussed the mechanical characteristic of the Mg-2%Zn alloy via MDF. The findings demonstrate that the Mg-2%Zn alloy with 3-passes of MDF at 280 °C possesses the highest YS and UTS, reaching 152 and 238 MPa, respectively. With a further increase to 5-passes MDF, the elongation is improved to 21%, whereas YS and UTS fall to 123 and 196 MPa, respectively. After 3-passes, it is attributed to the alloy's strain hardening and grain refining. Twin density is reduced, but DRX increases during the 5-passes of the MDF, changing the texture. As a result, the strength of Mg-2%Zn alloy decreases, and elongation increases gradually with more MDF passes. Moreover, ball burnishing can enhance the mechanical characteristics of Mg-Zn alloy.

Meanwhile, Bahmani et al^[65] used MDF to achieve a high-strength magnesium alloy. It is found that after MDF at 220 and 300 °C, YS increases from 168.12 MPa to 202.72 and 174.11 MPa, and UTS increases from 190.19 MPa to 241.01 and 223.21 MPa, respectively. This is mainly because the deformed grains are refined and more evenly distributed after forging, and the properties are continuously improved. However, with the increase in temperature, the grain size increases, and second phase Mg₂Ca is gradually dispersed, so the strength decreases. Subsequently, Gerashi et al^[66] investigated the improvement in strength of Mg-4Zn-0.3Sr prepared by MDF. Research results point out that after the MDF process, the grain size decreases from 57.1 μm to 9.2 μm , and ultimate shear strength (USS) increases by 15 MPa. It is explained by the fact that after 6-passes of MDF, considerable grain refinement has been accomplished. In the secondary stage, the microstructures are finer and more uniformly distributed following the MDF process. Besides, when MDF is carried out at a high temperature (280 °C), the dendritic microstructure is vanished. Additionally, Huang et al^[67] analyzed the medical Mg-Gd-Y-Zn-Ag-Zr MDFed parts with inhomogeneous microstructure and mechanical anisotropy. As shown in Fig.4, there are more tension twins in the center, which induce more dynamic recrystallization. Thus, grains in the center are finer than those in the edge. Also, there are different deformation degrees and dynamic recrystallization degrees, and the size distribution is uneven. In the center and the edge, the YS is 295 and 234 MPa, the UTS is 364 and 335 MPa, and the elongation is 4.8% and 5.2%, respectively. This is primarily caused by the dynamic precipitation of the β phase, which is mainly dispersed in the DRXed grain boundaries, and limits grain expansion via the Zener-pinning effect. Thus, the alloy's strength after MDF is increased, and its strength change meets the initial implantation requirements, while its strength loss and early failure need to be verified. Till now, the forging process

requires a high mechanical performance, by which its production parts bear a high mechanical load, so it is vulnerable to harm. As a result, it is essential to be aware of its potential safety risks.

1.3 Extrusion deformation

Compared with the above two deformation methods, the extrusion process owns a three-dimensional stress state and has more advantages for plastic working. It can enable the metal to give full play to its maximum shaping, improve its UTS, reduce its distortion, and even fracture after implantation. For example, Kang et al^[68] assessed the Mg-Zn-Y-Nd alloy's strength after the hot extrusion. The findings demonstrate that after extrusion, the YS and UTS increase from 118 and 126 MPa to 250 and 290 MPa, respectively. This is primarily because hot extrusion brakes up the eutectic and block phases into smaller pieces and refines the grains, which improves particle strengthening and synergetic deformation and enhances strength. Moreover, the alloy that has been hot extruded and subsequently heat-treated has the finest cytocompatibility. Panemangalore et al^[69] studied the mechanical characteristics and microstructure of extruded Mg-Zn-Ca-Er alloys for bio-medical applications. The outcomes demonstrate a rise in the YS and the UTS, reaching 128 and 225 MPa, respectively. This is mainly caused by the uniformly distributed secondary phases of the MgZn₂ type that is formed during hot extrusion, and the grains are refined. Moreover, due to the effect of Er element on particle strengthening, the Mg-Zn-Ca-Er alloy demonstrates the maximum strength.

Du et al^[70] researched the microstructure and mechanical property of the Mg-Zn-Y-Nd alloy with various extrusion ratios and extrusion passes. Research results indicate that as the extrusion ratio increases from 7 to 14 at 460 °C, the tensile yield strength (TYS) and the UTS decrease from 191 and 258 MPa to 138 and 235 MPa, respectively. With the increase in extrusion passes, the TYS and UTS increase significantly to 297 and 320 MPa, respectively. It is mainly due to the precipitation strengthening of Mg-Zn-Y-Nd alloy, since the secondary phases are refined by the increase in extrusion ratio based on Eq. (5). Meanwhile, because of continued dynamic recrystallization, the grains and precipitates are refined through many extrusion passes. With expanding the extrusion pass, the secondary phases and grains are refined, increasing the strength.

$$\Delta\sigma_{ps} = M \frac{Gb}{2\pi\sqrt{1-\nu}} \cdot \frac{1}{d\sqrt{\frac{\pi}{4f-1}}} \ln \frac{d}{b} \quad (5)$$

Liu et al^[71] pointed out the role of extrusion temperature and extrusion ratio on the mechanical and microstructural characteristics of biodegradable Mg-Zn-Gd-Y-Zr alloy. According to the findings, when the extrusion temperature increases, the alloy's mechanical characteristics at $\lambda=6$ firstly increase and then decrease. The UTS and YS are 290.1 and 262.5 MPa, respectively at 340 °C, at which the strength reaches the maximum. The alloy's strength tends to decline as the temperature increases at an extrusion ratio of 12. The YS

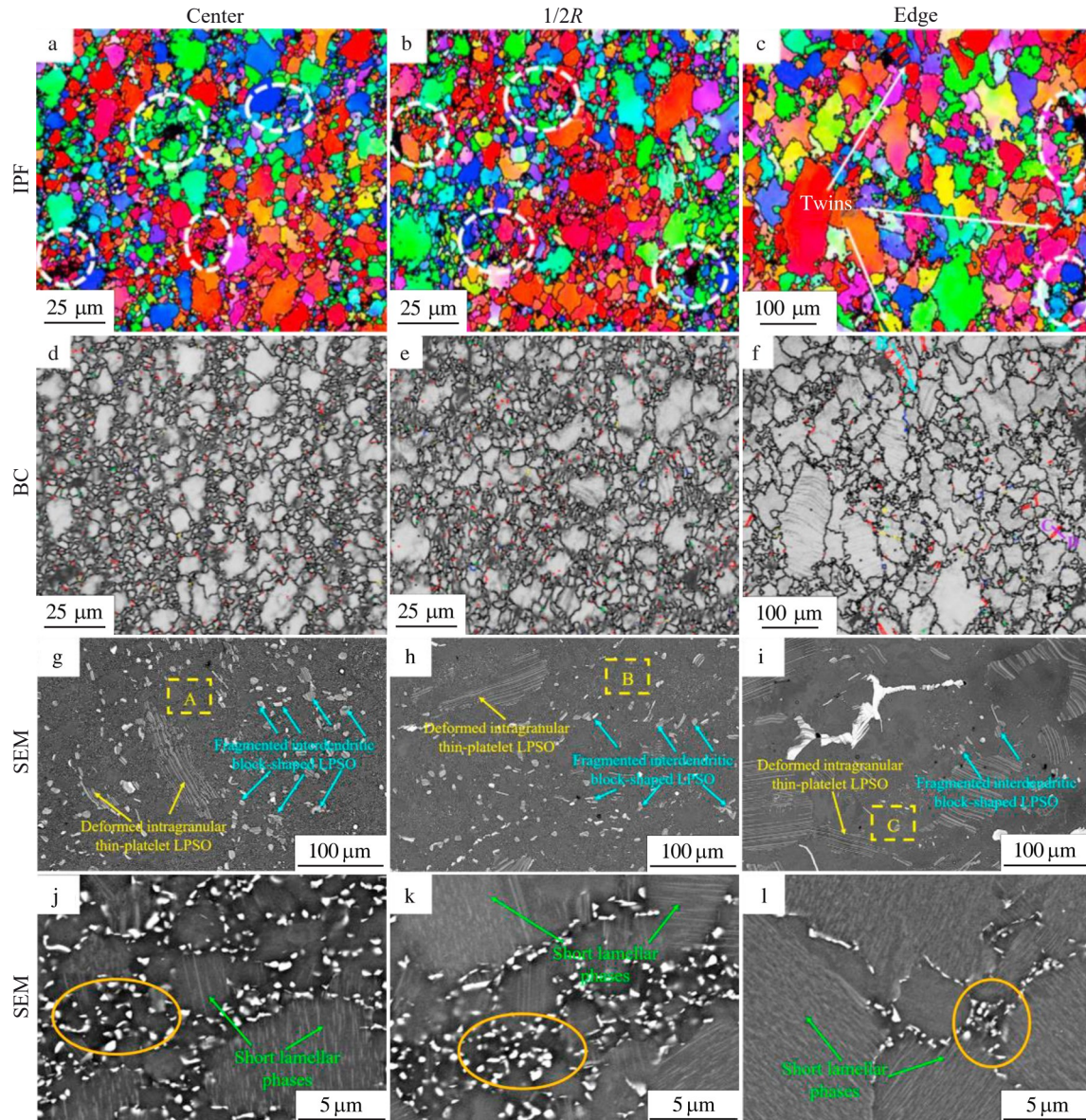


Fig.4 Microstructures of inverse pole figure (IPF) color images and Kikuchi band contrast (BC) maps of the MDFed medical Mg-Gd-Y-Zn-Ag-Zr alloys in the center (a, d), 1/2R (b, e), and edge (c, f) regions; SEM micrographs of the MDFed Mg-Gd-Y-Zn-Ag-Zr samples: (g) center, (h) 1/2R, and (i) edge; enlarged images of A (j), B (k), and C (l) regions in Fig.4g, 4h and 4i, respectively^[67]

is 234.4, 233.6, 194.3, and 182.1 MPa at 320, 340, 360, and 380 °C, and the UTS is 270.1, 268.3, 245.5, and 228.2 MPa, respectively. They found that when the temperature is 340 °C, the bimodal grain structure appears at a lower extrusion ratio, and complete dynamic recrystallization occurs at a higher ratio (as shown in Fig.5). The alloy extruded at $\lambda=6$ exhibits inhomogeneous dislocation and larger dislocation densities in the unDRXed regions.

Compared with common extrusion, the equal channel angular extrusion (ECAP) deformation process has large plastic deformation. It can not only reduce the grain size and homogenization of the microstructure of biomaterials, but also reduce the texture generated in the previous extrusion process, significantly improving the comprehensiveness of medical magnesium alloys, and continuously improving their

biodegradability and support performance.

For example, Martynenko et al^[72] examined the mechanical characteristics of degradable Mg alloy prepared by ECAP. The findings show that after ECAP, in comparison to the initial state, the YS and UTS increase from 92 and 194 MPa to 106 and 215 MPa, respectively, because the ECAP process of the Mg-Zn-Ca sheet gives rise to grain refinement from initial values of 106.0 μm to 4 and 8 μm in transversal and longitudinal cross-sections, respectively. Huang et al^[73] studied the effect of ECAP on microstructure and mechanical properties of Mg-Ca-MgO composite. The results indicate that after the 4th ECAP pass on the composite, the highest UTS of 161.1 MPa, TYS of 124.7 MPa, and ductility of 4.3% can be obtained, because ECAP process induces severe plastic deformation, resulting in grain refinement and grain size

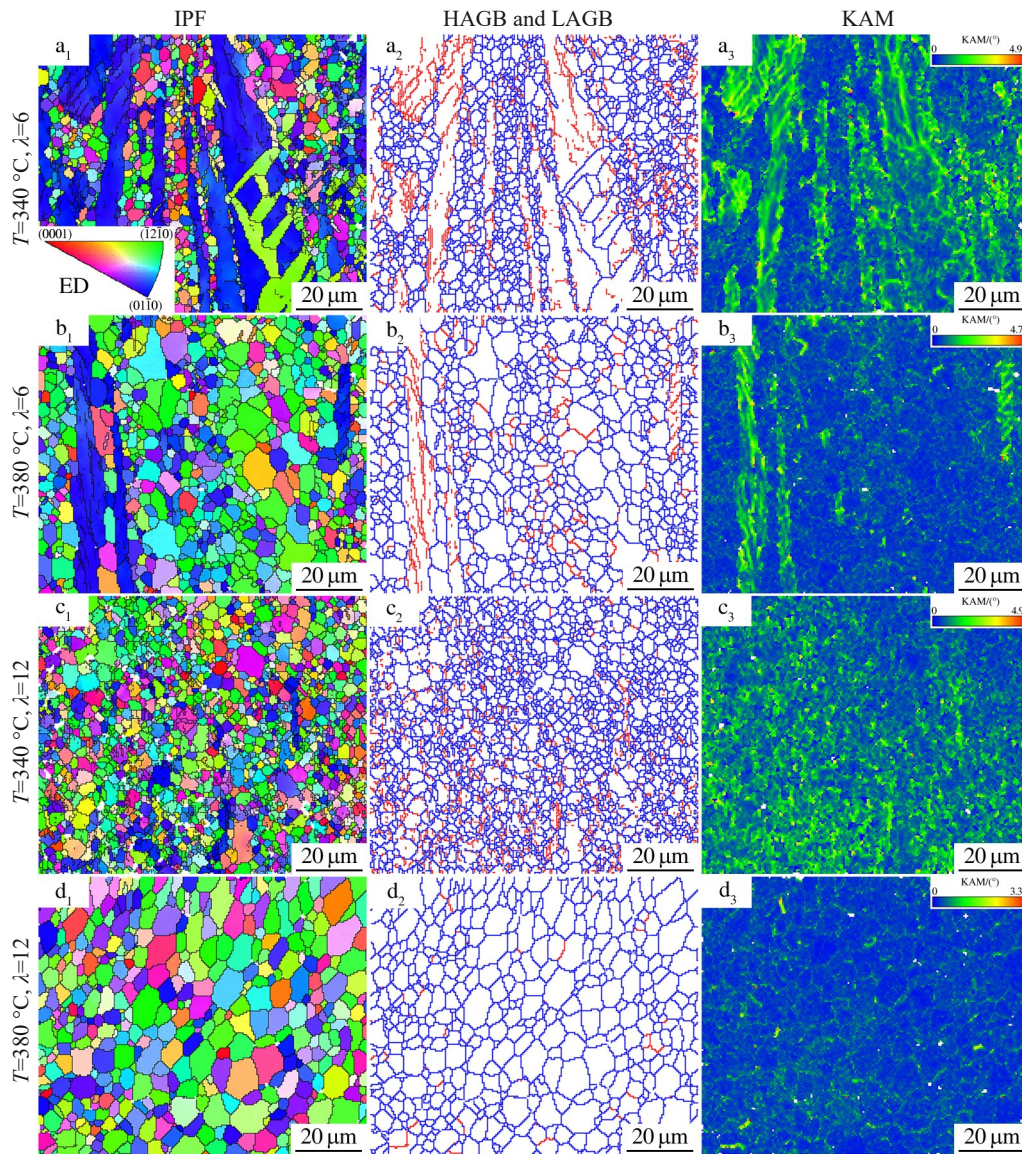


Fig.5 EBSD results of the extruded samples: (a₁-a₃) $T=340\text{ }^{\circ}\text{C}$, $\lambda=6$; (b₁-b₃) $T=380\text{ }^{\circ}\text{C}$, $\lambda=6$; (c₁-c₃) $T=340\text{ }^{\circ}\text{C}$, $\lambda=12$; (d₁-d₃) $T=380\text{ }^{\circ}\text{C}$, $\lambda=12$ ^[71]

reduction. The smaller grain size inhibits dislocation motion and enhances mechanical strength.

Subsequently, Bryła et al^[74] investigated the microstructure characteristics and mechanical behavior of Mg-Ag alloys treated by ECAP. These findings pointed out that after one-pass ECAP, the YS of the alloy is increased from 30 MPa to 45 MPa, and compressive strength is increased from 220 MPa to 300 MPa. After double equal-channel angular pressing (D-ECAP), the YS and compressive strength are further increased to 62 and 325 MPa, respectively, since ECAP can achieve significant grain refinement, from 350 μm to 38 μm (after one-pass) and even 15 μm (after two-passes). Also, after one-pass of ECAP, there are deformation twins, and after D-ECAP at the lowest temperature, the grains are refined. Moreover, the mechanical characteristics are unquestionably improved by the nano-sized Mg₄Ag particles. On this basis, Horky et al^[75] enhanced the mechanical characteristics of the Mg-Zn-Ca alloy through D-ECAP. Research results point out that with

the reduction in deformation temperature to 280 $^{\circ}\text{C}$, compared with conventional extrusion, YS rises from 225 MPa to 372 MPa, and tensile strength rises from 256 MPa to 375 MPa. It is because the area fraction of large grains decreases with increasing the number of passes, while the grain size decreases with decreasing the D-ECAP temperature. Thus, the strength is greatly improved. Additionally, the alloy that has undergone D-ECAP processing is excellent for biomedical applications as an absorbable component for osteosynthesis implants, due to its improved mechanical properties and low degradation rate. Till now, the extrusion process can produce medical products such as tubes and rods, whose profiles have complex shapes, and the product size is accurate. However, the metal consumption of the process is large, and the microstructure and properties of the alloy obtained are uneven, which requires further treatment by other methods.

1.4 High-pressure torsion

Compared with three kinds of deformations above, high-

pressure torsion (HPT) is another severe plastic deformation process. It can refine the size of metal particles and the second phases, and obtain medical magnesium alloy composites with high plasticity and strength. For example, Ahmadkhaniha et al^[76] studied the impact of HPT on microstructure characteristics and mechanical behavior of cast pure Mg. Results reveal that when as-cast pure Mg is treated by HPT for 1 or 5 turns, the YS rises by roughly 7 times. This is caused mainly by the fact that the grain size is refined after only one turn of processing. The microstructure becomes more homogeneous after 5 turns. Additionally, to describe the degradation behavior in vivo and in vitro, extra tests were required. On this basis, Li et al^[77] revealed the change in mechanical properties of pure Mg by HPT. The findings demonstrate that after HPT, the YS and UTS of pure Mg are significantly improved from 20 and 80 MPa to 117 and 160 MPa, respectively. This is caused by HAGBs, which lead to dynamic recrystallization and continuous refining of the grains. Also, the dislocation density gradually increases in the grains, so HPT considerably improves the mechanical characteristics. Additionally, even though HPT enhances the rate of in vitro degradation of HPTed pure Mg, animal testing and cell viability tests validate the high biocompatibility of substances.

Li et al^[78] studied the mechanical properties of ZEK100 by HPT. The results show that after 5 turns of HPT, the tensile strength is increased from 274.6 MPa to 339.3 MPa. Also, after the HPT treatment for 5 turns at a pressure of 6 GPa, the alloy's hardness becomes homogeneous. This is primarily the outcome of the HPT processing, which reduces the grain size and increases the number of twins, giving the material a homogenous microstructure and increasing its strength. Additionally, HPT-plentiful ZEK100's refined grains, twins, and grain boundaries offer more HA crystal nucleation sites, expanding the range of biological applications for magnesium alloys.

Subsequently, Li et al^[79] discussed HPT nanocrystalline Mg-Zn-Y alloy's mechanical characteristics and microstructure. Research results show that the hardness increases from 421.4 MPa to 529.2 MPa after 7 turns, and there is a rising tendency for the hardness toward the edge. This is primarily caused by the precipitation of nano-sized MgZn and MgZn₂ and the breakage of finer W(Mg₃Y₂Zn₃) phase particles, which accelerates dislocation development and grain refinement of the Mg-Zn-Y alloy after HPT processing. Also, the HPT processing successfully promotes the dissolution of the nanoscale MgZn and MgZn₂ phases. Moreover, Mg-Zn-Y alloy has excellent strength and hardness after it is implanted into the human body, and it is not easy to deform, such as bending and torsion. Li et al^[80] revealed the mechanical characteristics of pure Mg processed by HPT. Research results demonstrate that the YS of the 293 K-samples rises to 112, 132, and 148 MPa with increasing the numbers of HPT turns to 1/8, 1, and 10, at which the YS of the 423 K-alloys is 118, 112, and 113 MPa, respectively, remaining reasonably stable. This is caused by bimodal microstructures with fine grain

sizes after 10 turns of HPT processing. At 293 K, the strain accumulation gradually refines the microstructure, and when the rotation increases to 10 turns, dynamic recrystallization takes place. Therefore, refined grains produce grain boundary strengthening, and thus the strength is continuously improved.

Additionally, Zhang et al^[81] discussed the microstructure of Mg-Zn-Ca alloy that has undergone HPT. Research results show that after HPT, the alloy has an uneven surface stress distribution, and the stress in the edge area is higher than that in the central area. The surface stress decreases initially as the number of second phases increases. Subsequently, Horky et al^[82] adopted HPT to strengthen biodegradable Mg-Zn-Ca alloys. The findings demonstrate that HPT enhances the YS from 64 MPa to 158 MPa and the tensile strength rises from 184 MPa to 242 MPa. It is primarily because HPT-induced grain refinement boosts the materials' hardness and strength. Moreover, after HPT during heat treatment, the densely packed planes create agglomerates and dislocation loops that serve as barriers to dislocation movement. Thus, hardness and YS increase noticeably. These treated alloys are used more frequently as biodegradable load-bearing medical implants because of this novel hardening process. Till now, HPT has the characteristics of fine grain and uniform deformation. However, it can only produce small volumes of fine grains, and it is still complicated to prepare large-size samples. Therefore, the application of HPT is constrained due to the inability to conduct large-scale production.

2 Summary

According to the findings of previous studies, the mechanical characteristics statistics of Mg alloys in various states are summarized in Fig. 6^[83-92]. Based on the statistical-graph data, researchers can carry out appropriate hot deformation processes for different alloys. It can meet the performance requirements of specific parts and corresponding medical application effects.

Meanwhile, deformation processing can promote the formation of dense oxide film-layer on the surface by grain refinement, crushing second precipitations and decreasing the microstructure defects, thereby reducing the micro-galvanic corrosion and improving the corrosion resistance of medical Mg alloy^[93-94]. Even though the current thermal deformation processing can significantly improve the stability of Mg alloy implants, it not entirely solves the problem of the durability of the implanted metal.

3 Future Prospective

1) The healing of the damaged organ not only needs to maintain the material integrity and mechanical requirements, but also needs to consider that the corrosion products from the corrosion reaction must not exceed the body's absorption threshold. Thus, it is necessary to regulate the influence of corrosion products through comprehensive in vivo and in vitro experiments.

2) Aiming at the uncontrollable release rate and mechanical

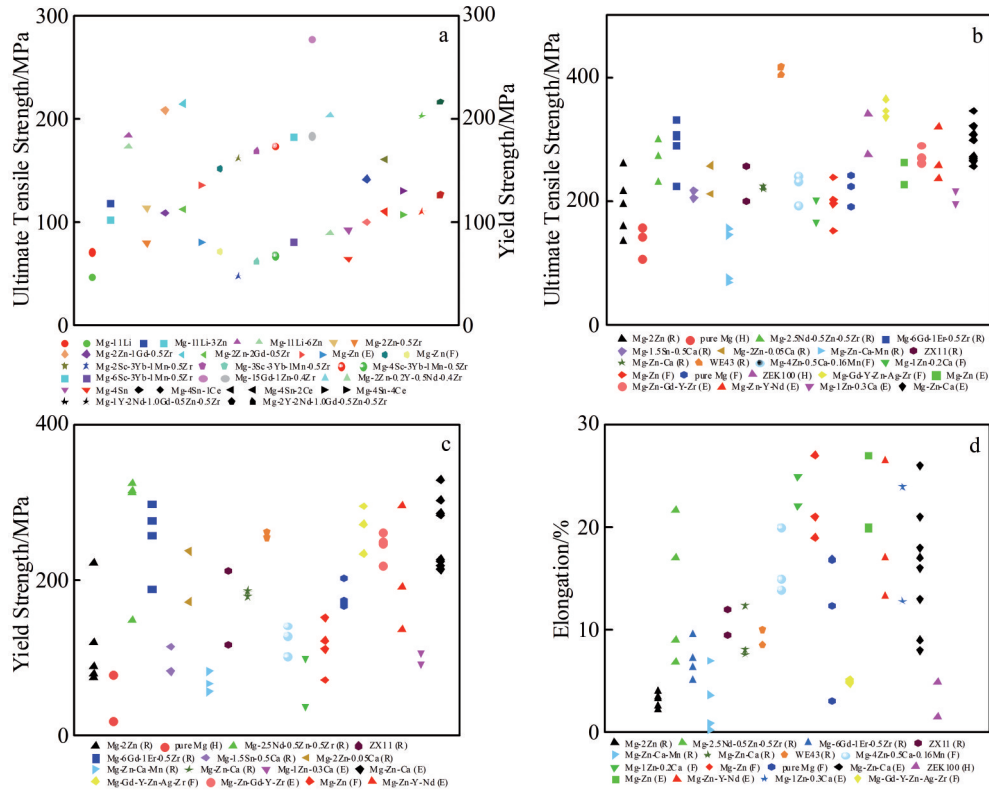


Fig.6 Mechanical properties of Mg alloys under different states: (a) UTS and YS in as-cast state^[54,64,83–86,89–91], (b) UTS^[54–55,57–60,62–65,67,70–72,75,77–78,87–88,92], (c) YS^[54–55,57–60,62–65,67,70–72,75,77,92], and (d) elongation^[54–55,58–60,62–65,67,70,72,75,78,87,92] (R: as-roll; F: as-forged; E: as-extruded; H: high-pressure torsion)

attenuation law of Mg^{2+} ions after implantation in vivo/vitro, and to fully realize the control of the entire process of medical magnesium alloys, more studies are required.

3) Till now, single hot deformations show remarkable limitations, which cannot fulfill the demanding in vivo implantation standards. Thus, to achieve excellent strength and corrosion fatigue, the combined action mechanisms of hot deformation, micro-composite addition, and surface alteration must be investigated.

References

- Bulla A, Wu K L, Shen C. *Materials Science and Engineering A*[J], 2023, 862: 144462
- Tanji A, Feng R, Lyu Z Y et al. *Corrosion Science*[J], 2023, 210: 110828
- Wang A G, Venezuela J, Dargusch M S. *Progress in Organic Coatings*[J], 2023, 174: 107301
- Rybalchenko O, Anisimova N, Martynenko N et al. *Materials*[J], 2023, 16(1): 45
- Qiang Meng, Yang Xirong, Liu Xiaoyan et al. *Rare Metal Materials and Engineering*[J], 2023, 52(5): 1673
- Peng W P, Chen Y Z, Fan H D et al. *Materials*[J], 2023, 16(2): 682
- Kuji C, Soyama H. *Metals*[J], 2023, 13(1): 181
- Roman A M, Voiculescu I, Cimpoesu R et al. *Crystals*[J], 2023, 13(1): 109
- Wang Q, Telha W, Wu Y G et al. *Journal of Clinical Medicine*[J], 2023, 12(2): 444
- Jana A, Das M, Balla V K. *Journal of Biomedical Materials Research*[J], 2022, 110(2): 462
- Kumar R, Katyala P. *Materials Today*[J], 2022, 56: 2443
- Li D, Zhang D C, Yuan Q et al. *Acta Biomaterialia*[J], 2022, 141: 454
- Pradeep N B, Rajath-Hegde M M, Manjunath-Patel G C et al. *Journal of Materials Research and Technology*[J], 2022, 16: 88
- Khrustal'ov A P, Akhmadieva A, Monogenov A N et al. *Metals*[J], 2022, 12(2): 206
- Kumar P, Jain N K, Jaiswal S et al. *Journal of Materials Research and Technology*[J], 2023, 22: 541
- Zhang Y, Cao J, Lu M M, et al. *Bioactive Materials*[J], 2023, 22: 225
- Li H Y, Qin Z N, Ouyang Y Q et al. *Journal of Alloys and Compounds*[J], 2022, 909: 164694
- Tong X, Han Y, Zhou R Q et al. *Acta Biomaterialia*[J], 2023, 155: 684
- Venkateswarlu B, Sunil B R, Kumar R S. *Materialia*[J], 2023, 27: 101680
- Han Z J, Guo H J, Zhou Y F et al. *Metals*[J], 2022, 12(4): 545
- Ahmady A R, Ekhlasi A, Nouri A et al. *Smart Materials in Manufacturing*[J], 2023, 1: 100009

- 22 Sui B Y, Lu H, Liu X et al. *Journal of Materials Science & Technology*[J], 2023, 140: 58
- 23 Schmidt J, Pana I, Bystrova A et al. *Colloids and Surfaces B: Biointerfaces*[J], 2023, 222: 113087
- 24 Baigonakova G, Marchenko E, Zhukov I et al. *Vacuum*[J], 2023, 207: 111630
- 25 Kennedy Z E, Shivappa D, Mohan S. *Materials Today*[J], 2022, 55: 470
- 26 He Junguang, Xu Dazhao, Wen Jiuba et al. *Rare Metal Materials and Engineering*[J], 2022, 51(2): 474
- 27 Chen J X, Xu Y, Kolawole S K et al. *Materials*[J], 2022, 15(14): 5031
- 28 Liu T, Chen X, Venezuela J et al. *Journal of Magnesium and Alloys*[J], 2024, 12(3): 1026
- 29 Ma Y C, Talha M, Wang Q et al. *New Journal of Chemistry*[J], 2022, 36: 4436
- 30 Guo Y T, Li G Y, Xu Z Z et al. *ACS Applied Bio Materials*[J], 2022, 5(4): 1528
- 31 Motallebi R, Savaedi Z, Mirzadeh H. *Journal of Materials Research and Technology*[J], 2022, 20: 1873
- 32 Nasution A K, Hermawan H. *Advanced Structured Materials*[J], 2016, 58: 127
- 33 Han H S, Loffredo S, Jun I D et al. *Materials Today*[J], 2019, 23: 57
- 34 Wang Q, Fang G, Zhao Y H et al. *Applied Sciences*[J], 2018, 8(12): 2461
- 35 Li J L, Qin L, Yang K et al. *Journal of Materials Science & Technology*[J], 2020, 36: 190
- 36 Chen C X, Chen J H, Wu W et al. *Biomaterials*[J], 2019, 221: 119414
- 37 Marchenko E, Baigonakova G, Khrustalev A et al. *Materials Chemistry and Physics*[J], 2023, 295: 126959
- 38 Singh N, Batra U, Kumar K et al. *Bioactive Materials*[J], 2023, 19: 717
- 39 Jamel M M, Lopez H F. *Metals*[J], 2022, 12(1): 85
- 40 Kalayeh P M, Malekan M, Bahmani A et al. *Journal of Alloys and Compounds*[J], 2022, 927: 166939
- 41 Ma D Q, Yuan S, Luan S Y et al. *Journal of Materials Research and Technology*[J], 2022, 21: 1643
- 42 Lv T, Jiang Y W, Chen J Q et al. *Materials Today Communications*[J], 2022, 33: 104135
- 43 Chaudrya U M, Farooqb A, Malik A et al. *Materials Technology*[J], 2022, 37(12): 2230
- 44 Gaalen K V, Quinn C, Benn F et al. *Bioactive Materials*[J], 2023, 21: 32
- 45 Peng X, Liu W C, Wu G H et al. *Journal of Materials Science & Technology*[J], 2022, 99: 193
- 46 Zerankeshi M. M, Alizadeh R, Gerashi E et al. *Journal of Magnesium and Alloys*[J], 2022, 107: 1737
- 47 Mi J, Ma D Q, Luan S Y et al. *Journal of Materials Research and Technology*[J], 2023, 22: 1533
- 48 Zhang H F, Ding Y T, Li R M et al. *Materials Science and Engineering A*[J], 2022, 853: 143733
- 49 Zhang Y, Li J Y, Liu Y et al. *Materials Characterization*[J], 2020, 165: 110368
- 50 Liu Y, Zhang Y, Zheng R N et al. *Materials Characterization*[J], 2021, 174: 111034
- 51 Zhang Yuan, Liu Wei, Liu Yun et al. *Rare Metal Materials and Engineering*[J], 2023, 52(9): 3065
- 52 Wang W H, Wu H L, Zan R et al. *Acta Biomaterialia*[J], 2020, 107: 349
- 53 Wang S H, Ma J F, Yang J L et al. *Journal of Materials Research and Technology*[J], 2021, 14: 2124
- 54 Wang W H, Blawert C, Zan R et al. *Bioactive Materials*[J], 2021, 6(12): 4333
- 55 Liu K, Lou F, Yu Z J et al. *Journal of Alloys and Compounds*[J], 2022, 893: 162213
- 56 Deng B, Dai Y L, Lin J G et al. *Materials*[J], 2022, 15(11): 3985
- 57 Mao G W, Jin X X, Sun J et al. *ACS Biomaterials Science & Engineering*[J], 2021, 7(6): 2755
- 58 Gungor A, Incesu A. *Journal of Magnesium and Alloys*[J], 2021, 9(1): 241
- 59 Hou R Q, Jose V H, Jiang P L et al. *Acta Biomaterialia*[J], 2019, 97: 608
- 60 Dargusch M S, Balasubramani N, Yang N et al. *Bioactive Materials*[J], 2022, 12: 85
- 61 Duley P, Bairagi D, Bairi L R et al. *Corrosion Science*[J], 2021, 192: 109860
- 62 Duley P, Sanyal S, Bandyopadhyay T K et al. *Materials Characterization*[J], 2021, 172: 110885
- 63 Merson D L, Brilevsky A I, Myagkikh P N et al. *Letters on Materials*[J], 2020, 10(2): 217
- 64 Ramesh S, Anne G, Bhat N et al. *Journal of Manufacturing Processes*[J], 2021, 68: 423
- 65 Bahmani A, Arthanari S, Seon S K. *Journal of Alloys and Compounds*[J], 2021, 856: 158077
- 66 Gerashi E, Alizadeh R, Mahmudi R. *Journal of Materials Research and Technology*[J], 2022, 20: 3363
- 67 Huang C, Liu C M, Jiang S N et al. *Materials Science and Engineering A*[J], 2021, 807: 140853
- 68 Kang Y Y, Du B N, Li Y M et al. *Journal of Materials Science & Technology*[J], 2019, 35(1): 6
- 69 Panemangalore D B, Shabadi R, Gupta M. *Metals*[J], 2021, 11(3): 519
- 70 Du B N, Hu Z Y, Wang J L et al. *Bioactive Materials*[J], 2020, 5(2): 219
- 71 Liu Y, Wen J B, Li H et al. *Journal of Alloys and Compounds*[J], 2022, 891: 161964
- 72 Martynenko N, Lukyanova E, Serebryany V et al. *Materials Letters*[J], 2019, 238: 218
- 73 Huang S J, Wang C F, Subramani M et al. *Journal of Composites Science*[J], 2023, 7(7): 292

- 74 Bryła K, Horky J, Krystian M et al. *Materials Science and Engineering C*[J], 2020, 109: 110543
- 75 Horky J, Bryła K, Krystian M et al. *Materials Science and Engineering A*[J], 2021, 826: 142002
- 76 Ahmadkhaniha D, Huang Y, Jaskari M et al. *Journal of Materials Science*[J], 2018, 53: 16585
- 77 Li W T, Liu X, Zheng Y F et al. *Biomaterials Science*[J], 2020, 8: 5071
- 78 Li Q T, Ye W B, Gao H et al. *Materials & Design*[J], 2019, 181: 107933
- 79 Li Y S, Wang J H, Xu R. *Vacuum*[J], 2020, 178: 109396
- 80 Li Z L, Ding H, Huang Y et al. *Advanced Engineering Materials*[J], 2022, 24(10): 2200799
- 81 Zhang C Z, Guan S K, Wang L G et al. *Journal of Materials Research*[J], 2017, 32(6): 1061
- 82 Horky J, Ghaffar A, Werbach K et al. *Materials*[J], 2019, 12(15): 2460
- 83 Chen J X, Tan L L, Yu X M et al. *Journal of Materials Science & Technology*[J], 2019, 35(4): 503
- 84 Zhou T S, Liu Z H, Yang D L et al. *Journal of Alloys and Compounds*[J], 2021, 873: 159880
- 85 Fu P H, Wang N Q, Liao H G et al. *Transactions of Nonferrous Metals Society of China*[J], 2021, 31(7): 1969
- 86 Wang J F, Zhou H B, Wang L G et al. *Journal of Materials Science & Technology*[J], 2021, 35(7): 1211
- 87 Zareian Z, Emamy M, Malekan M et al. *Materials Science and Engineering A*[J], 2020, 744: 138929
- 88 Wang C M, Zeng L M, Zhang W L et al. *Materials Characterization*[J], 2021, 179: 111325
- 89 Li C Q, Deng B B, Dong L J et al. *Journal of Alloys and Compounds*[J], 2022, 895: 162718
- 90 Özarlan S, Şevik H, Sorar I. *Materials Science and Engineering C*[J], 2019, 105: 110064
- 91 Kang L, Zhang L, Wu G H et al. *Journal of Magnesium and Alloys*[J], 2019, 7(2): 345
- 92 Wang S H, Zhang W C, Wang H X et al. *Materials Science and Engineering A*[J], 2021, 803: 140488
- 93 Kiani F, Lin J, Vahid A et al. *Journal of Magnesium and Alloys*[J], 2023, 11(1): 110
- 94 Moreno L, Matykina E, Yasakau K A et al. *Journal of Magnesium and Alloys*[J], 2023, 11(3): 1102

热变形可生物降解镁基合金的微观组织特征和力学性能研究进展

张源^{1,2}, 杨煜卓¹, 刘芸^{1,2}, 刘薇¹, 田亚强^{1,2}, 陈连生^{1,2}

(1. 华北理工大学 冶金与能源学院, 河北 唐山 063210)

(2. 华北理工大学 现代冶金技术教育部重点实验室, 河北 唐山 063210)

摘要: 镁合金凭借与人骨相近的弹性模量、体内自发的可降解性及优异的生物相容性, 在生物医用领域表现出巨大的发展潜力。然而, 镁合金室温塑性成形差及绝对抗拉强度/屈服强度低, 限制了其广泛应用。热变形作为一种有效改善镁合金力学性能的方式, 具有细化晶粒及破坏连续大尺寸第二相等特征, 通过引入高密度位错进而显著提高材料强度和塑性。因此, 从热变形医用镁合金组织演变特征出发, 以变形方式为分类依据, 综述了近年来医用镁合金热变形的研究动态。概述了轧制、锻造、挤压、高压扭转等4种典型热变形工艺的差异性特征。在此基础上, 阐述了不同热变形工艺下医用镁合金的晶粒细化机制, 动态再结晶过程和位错增殖对力学性能的影响规律。进一步归纳了热变形医用镁合金微观组织结构及力学性能的本质关联。

关键词: 医用镁合金; 热变形; 第二相; 晶粒细化; 力学性能

作者简介: 张源, 男, 1988年生, 博士, 副教授, 华北理工大学现代冶金技术教育部重点实验室, 河北唐山063210, 电话: 0315-8805420, E-mail: zhangy130481@ncst.edu.cn